

# MICRO-553 Haptic Human Robot Interface

EMG Control Lab Specialisation Report  
 Supervised by: Evgenia Roussinova  
 June 21, 2021

Chuanfang NING    Dorian BIGNET  
 (sciper: 320662)    (sciper: 322826)

## I. INTRODUCTION

The aim of this specialization project is to design and implement a control strategy allowing a user to control the haptic paddle through the contraction of a muscle, which is recorded by electromyography (*EMG*). In Section II concepts about *EMG* signals are briefly introduced. The basic processing and filtering of raw *EMG* signal are discussed. The control strategies of haptic paddle using *EMG* data are explained, refined and evaluated by experiments. In Section III, three different application use cases of *EMG* control are introduced along with experiments. In Section IV, the potential and problems of *EMG* control method in prosthetics and other fields are discussed. A quick conclusion about this specialisation lab is reached in Section V.

## II. EMG CONTROL IMPLEMENTATION

### A. *EMG* Introduction

The *EMG* signal is a biomedical signal that measures electrical currents generated in muscles during its contraction representing neuromuscular activities [1]. Controlling haptic devices with *EMG* signal is interesting as it reflects the activities and intentions of muscles [2]. To acquire *EMG* signals of high fidelity usually a subtractor is used to detect the difference of signals from a pair of electrodes. As shown in Fig. 1, the detection electrodes are placed between one motor point and another along the direction of muscle fibers.

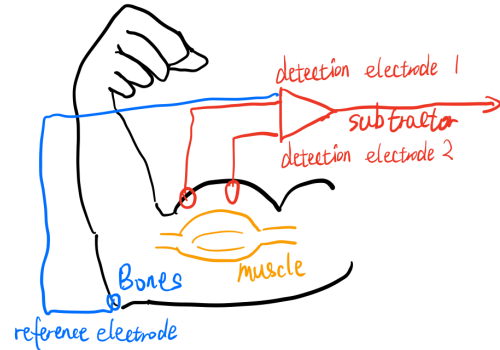


Fig. 1: Placement of electrodes

Besides the signal detection electrode, there is also a reference electrode attached to an electrically-unrelated tissue far away from the measure point to provide a common reference of signals.

The output signal of the subtractor goes through an ADC and feeds as input to the control board of haptic paddle. As shown in Fig. 2 are the *EMG* signals obtained from Dorian's Biceps Brachii on his right arm in still and contract state. The frequency spectrums of the *EMG* signals are shown as in Fig. 3. It can be seen that the main power of *EMG* signal concentrates in range  $10Hz$  to  $250Hz$ .

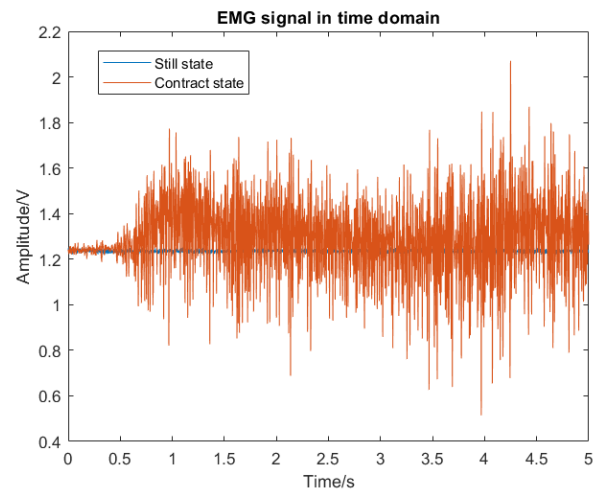


Fig. 2: *EMG* signal in time domain

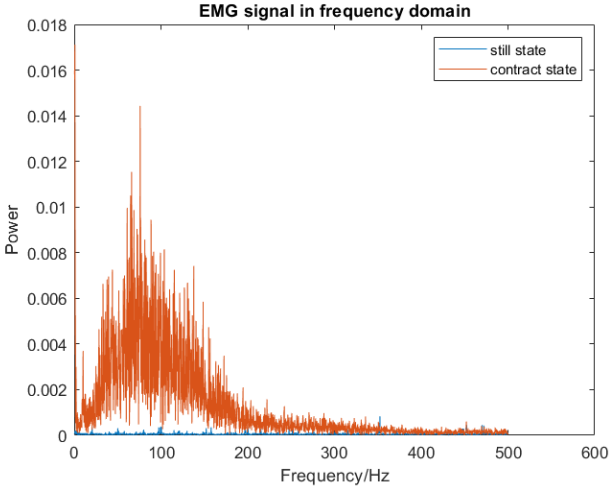


Fig. 3: EMG signal in frequency domain

### B. EMG Processing

The raw *EMG* signal is stochastic in nature. To obtain useful information from the signal, a low-pass filter with  $10Hz$  cut-off frequency and a high-pass filter with  $250Hz$  cut-off frequency are applied to extract the signal in the selected bandwidth discussed in the section above. The digital expression of the filters are shown as in Eqn. 1 and Eqn. 2 with  $\alpha = \frac{dt}{dt+\tau}$  for low pass filter and  $\alpha = \frac{\tau}{dt+\tau}$  for high pass filter. In the equation,  $x$  is the input signal,  $y$  is the filtered signal,  $dt$  is the sampling period and  $\tau$  is the *RC* constant calculated from cut-off frequency.

$$\text{Lowpass} : y[t] = y[t - 1] + \alpha(x[t] - y[t - 1]) \quad (1)$$

$$\text{Highpass} : y[t] = \alpha(y[t - 1] + x[t] - x[t - 1]) \quad (2)$$

As shown in Fig. 4 is the signal before and after applying the filters.

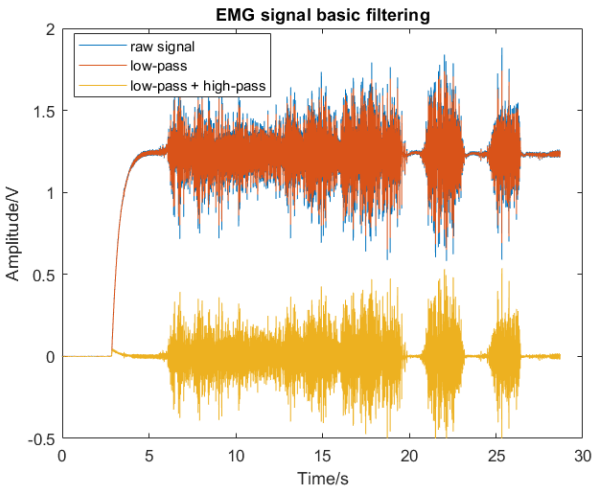


Fig. 4: EMG signal basic filtering

It can be seen that the filtered *EMG* signal is representative of a series of oscillations. The more the muscle contracts, the more power the oscillation has. To get the strength of muscle activity, a Root-Mean-Square(*RMS*) filter is applied to the signal filtered by the band-pass. The *RMS* filter takes the square root of the arithmetic mean of 100 consecutive squares of the values from band-pass filter. The digital expression of *RMS* is shown as in Eqn. 3, where  $x$  is the input signal from last filters,  $y$  is *RMS* the filtered signal and  $n$  is the *RMS* sampling window.

$$\text{RMS} : y[t] = \sqrt{\sum_{i=0}^{n-1} x \left[ \left\lfloor \frac{t}{n} \right\rfloor + i \right]^2} \quad (3)$$

As shown in Fig. 5 is the signal before and after applying the *RMS* filter.

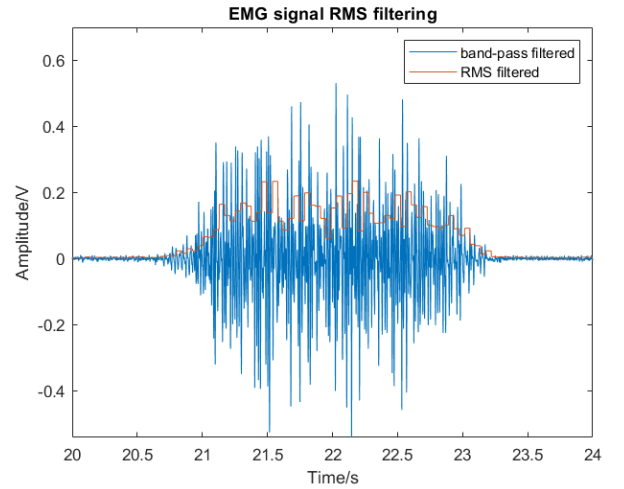


Fig. 5: EMG signal RMS filtering

Due to the fact that the *RMS* filter calculates the arithmetic mean of square root over a time window, the signals are made of sequences of small discrete steps. To remove the sharp edges on the signal, an additional low-pass filter with a cut-off frequency of  $2Hz$  is applied to smooth the signal. As shown in Fig. 6 is the signal before and after applying the low-pass filter.

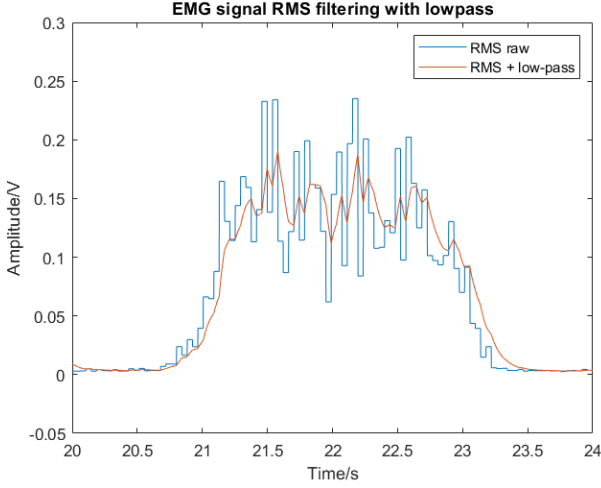


Fig. 6: EMG signal RMS filtering with lowpass

It can be seen that applying a low-pass on *RMS*-filtered signal would finally result in a smooth signal that could well represent the strength of muscle activity.

### C. EMG Control

In this section two control strategies are introduced to use the filtered signal from last section to control the haptic paddle in lab specialisation. Users can freely switch between the control modes in *GUI*.

1) *Position Control*: In the position control mode, the filtered *EMG* signal is mapped to a range of angles along the haptic paddle linearly as shown in Eqn. 4. The right boundary position of the paddle corresponds to filtered signal of 0V and the left boundary corresponds to the maximum filtered signal generated by the user noted  $EMG_{max}$ . This maximum value could vary from person to person. During experiments, it is observed that Dorian's right arm muscle generates signal up to 0.149V after filtering while Chuanfang's left arm muscle generates signal up to 0.090V after filtering. It is therefore considered necessary to re-calibrate the linear mapping when switching the user of the paddle.

$$pos_{star} = pos_r + (pos_l - pos_r) \left( \frac{EMG}{EMG_{max}} \right) \quad (4)$$

Whenever the target position updates in position control mode, the paddle uses the position *PID* controller introduced in Lab3 to reach the new target position.

2) *Torque Control*: In the torque control mode, the filtered *EMG* signal is mapped to a range of output torque from 0*N.m* to a maximum value (0.075*N.m* in experiments) linearly as shown in Eqn. 5. As there is no mechanical limits on paddle position, the paddle has

to be pushed against finger or wall while torque control mode is on.

$$torque_{tar} = torque_{max} \left( \frac{EMG}{EMG_{max}} \right) \quad (5)$$

### D. Tremor Rejection

It is observed during the test of position control that with linear mapping, it is hard for users to hold the paddle position as the paddle oscillates a lot during the whole experiment. This is due to the fact that the electrodes are pretty much sensitive to the change in *EMG* signals. Even if the user didn't intend to move the paddle, the tremor of muscle will incur tremor on the paddle.

To solve this problem, a new filter is introduced to improve the position control. This filter acts like a moving threshold that follows the filtered *EMG* signal. Only when there is an abrupt change in target position that overcomes this threshold, the new target is updated after attenuation. The logic of the moving threshold is shown as in Eqn. 6, where  $W$  is the window size of the moving threshold. With the moving threshold filter, the paddle could reject tremor of muscles in still state while remaining alert for muscle activity.

$$y[t + \Delta t] = \begin{cases} x[t] - W, & \text{if } x[t] > y[t] + W \\ x[t] + W, & \text{if } x[t] < y[t] - W \\ y[t], & \text{otherwise} \end{cases} \quad (6)$$

An example of filtering can be seen in Figure 7.

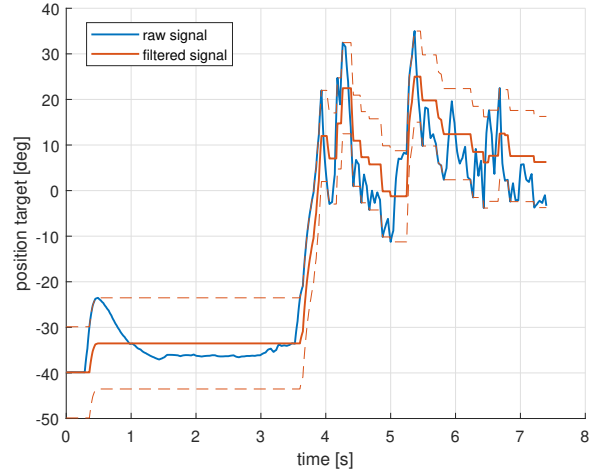


Fig. 7: Moving threshold filter effect

Remark that this new filter changes the maximum and minimum position values that can be reached by  $W$ , the filtering window. As a consequence,  $pos_r$  and  $pos_l$  are modified accordingly to counteract this effect in the filter equations presented previously.

### E. Positioning Experiment

Two groups of experiments are carried out in position control mode to evaluate the tremor rejection effect of the moving threshold filter. In the first group of experiments, Dorian and Chuanfang attempt to drive the paddle to three different target positions in a straight with direct linear mapping. In the second group of experiments, Dorian and Chuanfang attempt to drive the paddle to the same three targets with moving threshold filter enabled. The paddle positions are tracked and recorded in both groups of environments for further analysis. The target positions are  $3.25^\circ$ ,  $-9.75^\circ$  and  $16.25^\circ$ , which correspond to different grooves on the paddle surface. The experiment results are shown as in Fig. 8 and Fig. 9.

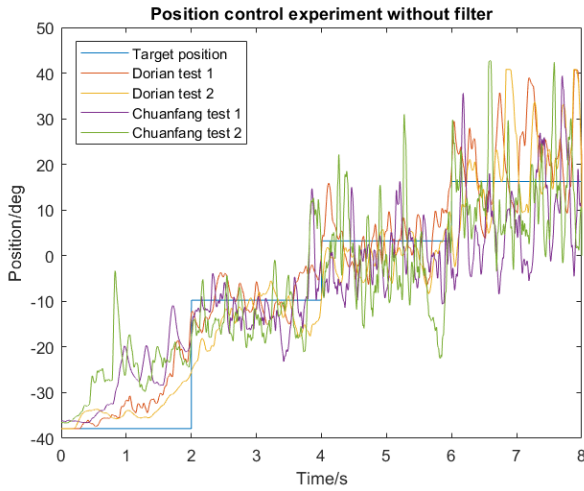


Fig. 8: Paddle position control results with direct linear mapping

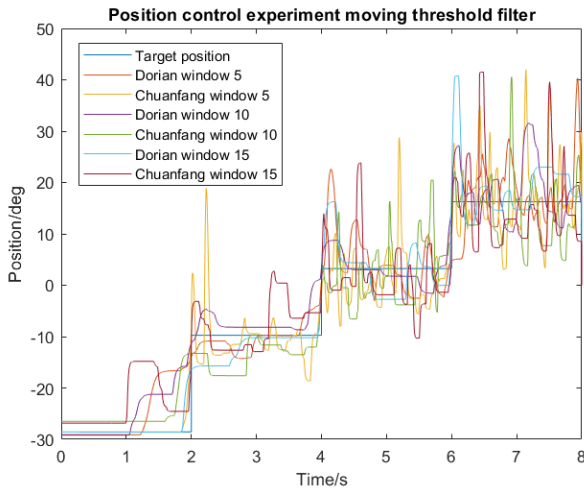


Fig. 9: Paddle position control results with moving threshold filter

To evaluate the stability of position control, the standard deviation of the error is examined. To evaluate the accuracy, the absolute value of average mean error is examined. The results are shown as in Tab. I.

Experiment	Std [deg]	Abs mean [deg]
Dorian no filter 1	7.0433	0.7281
Dorian no filter 2	5.8179	13.0067
Chuanfang no filter 1	8.2797	3.2246
Chuanfang no filter 2	9.0769	1.9108
Dorian W=5	5.5881	1.2096
Chuanfang W=5	5.6196	0.2683
Dorian W=10	4.4975	2.0949
Chuanfang W=10	5.6095	0.9492
Dorian W=15	4.8050	0.3023
Chuanfang W=15	6.8396	1.0889

TABLE I: Evaluation of position control performance

From plots and the table, it can be observed that applying a moving threshold filter significantly smooths the curves of paddle position and decreases the standard deviation of the error. Moreover, the bigger the window size  $W$  is, the more stable the paddle movement is. The absolute value of average mean error doesn't evolve consistently in the tests. This result is potentially because the *EMG* control is subtle in nature and the test subjects' small muscle activities would result in great errors. Not enough experiments have been done to eliminate this accidental error. However, it is observed in the experiments that once the test subject reaches the target position with a larger threshold window  $W$ , it would be much easier for the subject to hold at that position and to maintain a very low error rate. If the test subject doesn't manage to get to the target position in one muscle activity, the threshold window would make it much harder to make subtle changes on paddle positions, as even a small change would require a rather large variation in *EMG* signal to overtake the defined threshold window. All the more so the paddle behavior is now non-linear as it doesn't move until there is enough *EMG* power so the subject may intuitively deliver too much strength by impatience so it is hard to finely position the paddle.

As a conclusion, applying the moving threshold filter on top of linear mapping would significantly smooth the haptic paddle control and reduce tremors. On the other hand, a strong filter with a big threshold window would make subtle change in position much more difficult.

### III. APPLICATIONS

*EMG* control which has been implemented from now can have a lot of application fields. Three of them are going to be exposed in the following.

### A. Assistive Use Case

The very first application which has been tackled is the **Assistive application**. This can be very interesting in haptic interfaces and cobots which assist the human to make strength tasks easier. It has been seen that *EMG* control can be very stable thanks to the use of some filters. However, in this specific field, the goal is to reduce fatigue as much as possible while being extremely precise so an operator can use the interface for a long time period.

As a consequence, a new mapping of the muscle activity is required. The objective is to reach and to stabilize to a precise target (either position or force) at a fraction of the maximum *EMG* power so less fatigue may occur. As a consequence, the operator may be able to use the interface for a much longer time which is the main focus of this application. Note that only position control is studied in the following.

From now, only a linear mapping is available which is not really adapted to this use case. It has been seen previously that precision with linear mapping is lacking all the more so there is a risk to oscillate around the target as the operator has to keep a muscle activity in a small and specific window. A new muscle activity mapping is introduced: **saturation mapping**. The principle is extremely simple. A threshold ratio  $\gamma_{p,sat}$  (portion of  $EMG_{max}$ ) is defined so in the case where more muscle activity is provided, the target is saturated so the control is extremely precise and stable. Below this *EMG* threshold, a linear mapping is applied so the operator can still have a rather fine control in position. As a consequence, it looks clear that a balance is drawn between fatigue and control keenness. If the threshold is reduced, less fatigue may occur while the control window is smaller so the control is less fine. In addition, another activation threshold ratio  $\gamma_a$  can be implemented to avoid any unintentional movements. The saturation mapping is summarized in Figure 10 and expressed in Equation 7.

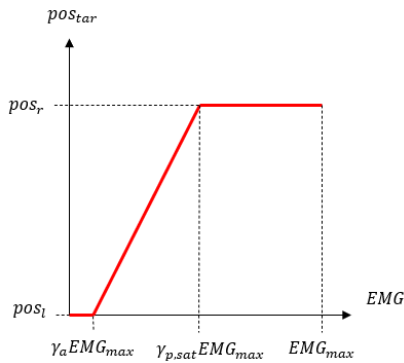
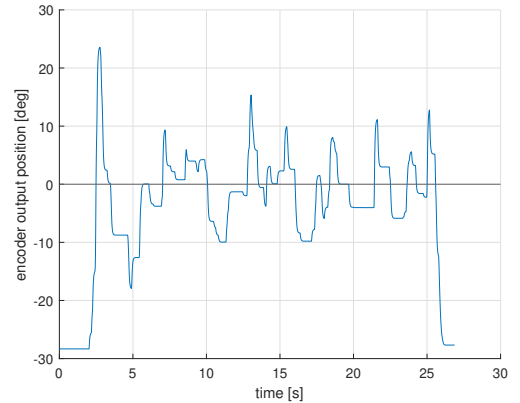


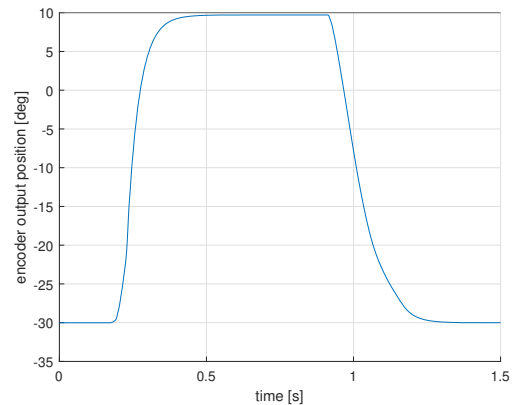
Fig. 10: Saturation Mapping Relation

$$pos_{tar} = \begin{cases} pos_l, & \text{if } EMG < \gamma_a EMG_{max} \\ pos_r, & \text{if } EMG > \gamma_{p,sat} EMG_{max} \\ \frac{EMG - \gamma_a EMG_{max}}{EMG_{max}(\gamma_{p,sat} - \gamma_a)} (pos_r - pos_l) + pos_l, & \text{otherwise} \end{cases} \quad (7)$$

Note that the effect of the moving threshold is also taken into account by modifying the  $pos_l$  and  $pos_r$  values accordingly as already discussed in previous sections. This new control strategy is implemented and is compared to the simpler linear mapping. A position experiment is done, with linear mapping first shown in Figure 11a and saturation mapping next shown in Figure 11b. The goal of this experiment is to reach a specific target and to compare the performances. For linear mapping, the target to reach is  $0^\circ$  which corresponds to half of  $EMG_{max}$  (as  $pos_l = -30^\circ$  and  $pos_r = 30^\circ$ ). In order to make the two experiments comparable, the muscle activity required to reach a  $10^\circ$  target with the saturation mapping is also half of  $EMG_{max}$  so  $\gamma_t = 0.5$ . Note that the moving threshold is enabled in the two experiments.



(a) Linear Mapping Experiment:  $0^\circ$  target



(b) Saturation Mapping Experiment:  $10^\circ$  target,  $\gamma_t = 0.5$

Fig. 11: Position experiments regarding the EMG mapping

It is clear that the new mapping strategy definitely solves some issues of the linear one previously exposed. The control is extremely precise and performances are mainly set by the *PID* controller. In addition, less fatigue can be felt as no energy is spent to continuously regulate the position which results in an oscillatory response with linear mapping. Lastly, the position is much smoother as well.

This mapping strategy is then extremely well adapted to assistance. The operator can well control the position with precision without oscillatory behavior while reducing fatigue.

### B. Rehabilitation Use Case

Another field of application of *EMG* control is rehabilitation. More specifically, it can be used to reinforce muscle fibers and to help for reinnervation after a stroke. This is a very complex process where haptics can be an interesting and perhaps efficient tool.

The patient can be asked to strengthen his muscle to reach a specific muscle activity measured with *EMG* electrodes. The signal can be used to move a paddle so the patient focuses on it and tries to reach a target position which corresponds to the expected muscle activity. The rehabilitation exercise is obviously adapted to the patient, depending on his pathology, so he can reach the goal. As a consequence, the patient will train his muscles which will become stronger and stronger. At first, the *EMG* control is very assistive and easy to move. It is then made harder and harder so more *EMG* power is required to reach the target so it is more challenging to the patient. This can be done with either linear mapping or saturation mapping. Parameters  $EMG_{max}$  and  $\gamma_t$  are increased step by step for that purpose. The advantage of this is that it can be well adjusted to the patient so the exercise is optimized and efficient.

Rehabilitation with *EMG* control can use the same basis than assistive applications previously exposed, but the objectives are extremely different. In rehabilitation, the goal is not to reduce fatigue. On the contrary, it is to solicit muscles in an efficient way to reinforce muscle fibers. Obviously, this is only possible when the patient still have the capability to use some muscles. As an example, this strategy is absolutely not adapted for paraplegics.

### C. Grasping Use Case

The last application field which is studied here is grasping thanks to *EMG* control. This is a very specific application which can be required in hand prosthesis. The objective is then to give the capability

to an amputee to grasp a fragile object such as a glass. This is a more complex strategy which requires both position and force control. Indeed, the patient may be able to close fingers so the latter are in contact with the object and in a second time, control and limit the force applied to the object so it doesn't slip or break.

1) *Control Strategy Description*: A new control strategy is required. The one which is studied here is the following and shown in Figure 12.

- At first, a position control with saturation mapping is applied. This is exactly what has been presented in previous sections.
- Next, once the *EMG* overtakes the saturation ratio  $\gamma_{p,sat}$ , the control switches into torque regulation. The torque is computed as a linear relation of the muscle activity and is saturated after a given relative threshold  $\gamma_{t,sat}$  in the remaining *EMG* range.

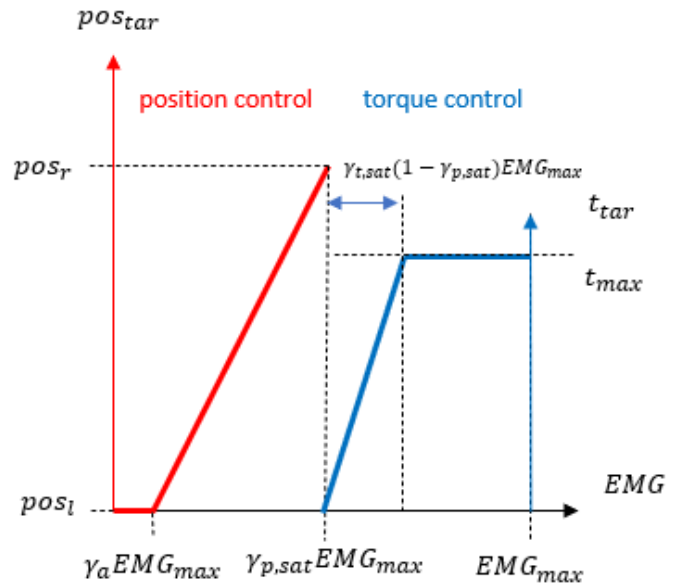


Fig. 12: Grasping control strategy

The equation for position control is exactly the same than in Eq. 7. In what concerns torque control for  $EMG \geq \gamma_{p,sat}EMG_{max}$ , Eq. 8 defines the relation used. Note that in this area, the *PID* controller is disabled.

$$t_{tar} = \begin{cases} t_{max}, & \text{if } EMG > EMG_{max}(\gamma_{t,sat}(1-\gamma_{p,sat}) + \gamma_{p,sat}) \\ t_{max} \left( \frac{EMG - \gamma_{p,sat}EMG_{max}}{EMG_{max}\gamma_{t,sat}(1-\gamma_{p,sat})} \right) & \end{cases} \quad (8)$$

As a consequence, the control is split in two parts. First, the operator closes the fingers and reaches a precise position by increasing his muscle activity. Next, the control switches into torque control so the amputee can regulate the torque linearly via *EMG* signal. The torque

is saturated to avoid breaking objects and to ensure the grasping while reducing fatigue for holding. This is extremely important as it is a daily life action so a rather low effort is preferable to improve comfort.

An experiment is done to study the fatigue performances with this specific control strategy. It is presented in next Section.

2) *Grasping Fatigue Experiment*: The fatigue regarding some control parameters and thresholds is assessed in an experiment for both Dorian and Chuanfang. The  $EMG_{max}$  parameter is fixed all throughout the experiments according to the operator. The goal is to hold torque saturation to simulate a daily use of the controller as long as possible. The *hold time* and *saturation time* are assessed and results are shown in Table II. An example of record can be seen in Figure 13.

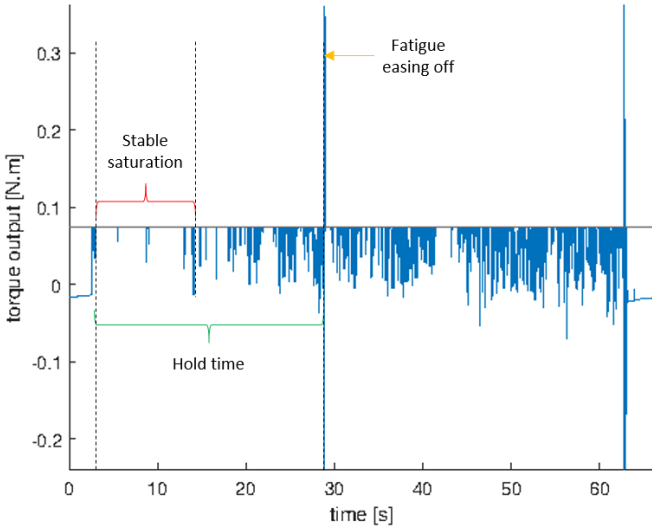


Fig. 13: Fatigue experiment measure (Dorian with torque saturation = 0.438)

The *stable saturation* time is defined as the time period during which the operator well stabilizes the torque to saturation by strengthening his muscle enough. The *hold time* is defined as the time duration during which the operator succeeds to stay in torque control mode so there is no strong and unexpected torque peaks. Indeed, when the operator releases too much the tension, the controller switches to position control so high torque peaks appear to compensate for the position of the paddle. This can be related to a fatigue easing off as the user starts releasing the muscle activity so the control becomes more and more oscillatory. In Figure 13, it is clear that the fatigue increases more and more all throughout the experiment.

Torque saturation	Hold Time		Stable Saturation	
	Dorian	Chuanfang	Dorian	Chaunfang
0.875	14.1s	4.4s	0.6s	0.5s
0.750	14.1s	4s	2.2s	1.1s
0.625	19.9s	3.6s	2.9s	1.7s
0.438	26s	8.2s	10s	2.4s
0.235	126s	15.7s	41s	2.5s

TABLE II: Fatigue Results

It looks clear that reducing the saturation ratios definitely helps to reduce fatigue. It sounds normal as less muscle activity is required to hold saturation. As a consequence, reducing the position threshold, which defines the beginning of the torque control, and the torque saturation ratio improves the holding time. However, it means that less working space is available for position control so it is rougher and less fine. This has been noticed during experiments. This can be a problem when considering grasping for instance as a rather fine control in position could be expected for a good daily comfort. This sounds incompatible with fatigue reduction so the choice of saturation ratios really come out of a balance and depends on the application.

3) *Possible Improvement*: Another control strategy may be preferable to counteract the issues previously exposed. The goal would be to increase the *EMG* working space of torque control while not encroaching on the position control one.

As a consequence, rather independent controllers could be an option with trigger conditions to switch between them. As an example, the initial mode could be position control. Either a saturation mapping or linear mapping can be used. A linear mapping sounds more adapted in this situation as it is possible that the object position is unknown so the controller doesn't know how much fingers should be closed. It is then more modular as there is no need to specify this beforehand. A saturation behavior will come out of the top-level control strategy.

Next, when a strong deceleration is detected or that the speed is suddenly close to zero, a collision is detected. A specific care has to be taken regarding the velocity as some bouncing behavior could appear. A strong unexpected deceleration sounds more adapted for collision detection in this specific application despite being much more susceptible to noise amplification. When a collision is detected, the controller switches into a saturation torque control with the full *EMG* space, from 0V to a threshold defined beforehand.

Lastly, when no muscle activity is applied, the controller can go back to position control to put an end to manipulation. As a consequence, the position control can be extremely fine while reducing fatigue in torque

control mode as both are rather independent one to another. At least, each *EMG* space is decoupled to the other which wasn't the case in the controller presented previously.

#### IV. DISCUSSION

- It has been seen that *EMG* control is extremely useful in a lot of application fields such as rehabilitation, cobots, prosthesis for example. However, it has been seen that this type of control is not very safe and positions are not very well controlled by the user in terms of precision, accuracy nor stability. Some mapping can help to improve these metrics but on the price of less modularity. As a consequence, the control strategies expressed in this project are not very well adapted to application with strong safety requirements such as surgery and teleoperation. A focus on the capacity of the user to finely control the trajectory is necessary which was not the main focus of this project. This is most certainly achievable but it sounds a rather difficult target and may have no strong interest. A more classic control with handles seems preferable for these types of applications.
- Note that the stiffness of the controller is mainly related to the position *PID* controller implemented. It is right that if the control doesn't stabilize position nor filter tremors, the stiffness can be theoretically reduced as the trajectory is much more oscillatory. However, it is extremely hard to define and to measure. All the more so the real stiffness of the controller is the same as it only tries to follow the oscillatory input of the muscle activity.
- The controllers presented in this project are patient-based. A calibration is required as the maximum muscle activity  $EMG_{max}$  has to be measured before running controllers.
- The advantage of *EMG* control is that a scaling factor either on position or torque is easily implementable. The torque can upscale or downscale so it is well designed for assistive cases or rehabilitation as an example.
- The grasping analysis has been done on the paddle which is not very well suited for that purpose. An adapted hand prosthesis would be an excellent haptic mechanism to test the implemented controller and to conduct reliable experiments. Moreover, the proposed grasping strategy shown in Section III-C3 sounds promising so further analysis of this controller is encouraged. The two grasping strategies can be compared one to another regarding fatigue, practicality and controllability.

- One additional question which is raised by this project is what is the influence of the haptic feedback on performances? All throughout the experiments, only a visual feedback of the paddle position via graphs or direct sight have been used. Other haptic feedback can be implemented such as vibrotactile feedback. It would be interesting to assess the influence of the feedback choice on metrics such as oscillations, precision and stability. It sounds clear that using a more complex feedback requires some training before getting used to it. As a consequence, assessing the evolution of performances with time can be as well an interesting analysis.

#### V. CONCLUSION

As a conclusion to this project, *EMG* control is a really promising control strategy which can be used in a lot of application fields. Some issues have to be tackled such as the rather oscillatory muscle activity. Depending on the application use case, reducing tremors, reaching precise position or torque values or saturating signals can be nice ways to reach impressive performances.

As an example, the moving filter introduced in Section II-D definitely rejects the tremors so the control is extremely smooth and looks natural but suffer from accuracy and controllability performances. Adding a saturation behavior on top of that can help to reach extremely precise target but the controllability of the interface is not improved as the operator can not well choose an intermediate position.

Another focus of this project is grasping. Results are really impressive and a clear conclusion on effect of saturation ratios regarding fatigue has been assessed. A brand-new and promising strategy is proposed to solve the main drawbacks of the implemented one, more especially regarding the *EMG* working spaces of either position and torque control which are not encroached one to another anymore.

#### REFERENCES

- [1] Reaz, Mamun Bin Ibne, M. Sazzad Hussain, and Faisal Mohd-Yasin. *Techniques of EMG signal analysis: detection, processing, classification and applications*. Biological procedures online 8.1 (2006): 11-35.
- [2] Song, Rong, et al. *Assistive control system using continuous myoelectric signal in robot-aided arm training for patients after stroke*. IEEE transactions on neural systems and rehabilitation engineering 16.4 (2008): 371-379.
- [3] De Luca, Carlo J. *Surface electromyography: Detection and recording*. DelSys Incorporated 10.2 (2002): 1-10.